Detailed Kinetic Modeling of PAH Growth and Soot Formation in Shock Tube Pyrolysis of Benzene and Ethylene

G. L. Agafonov[1], I. Naydenova[2], M. Nullmeier[2], P. A. Vlasov[1], and J. Warnatz[2]

[1]Semenov Institute of Chemical Physics, Russian Academy of Sciences, Kosygin str. 4, 119991 Moscow, Russia, E-mail: iz@chph.ras.ru

[2]IWR, Universität Heidelberg, Im Neuenheimer Feld 368, D-69120 Heidelberg, Germany, E-mail: warnatz@iwr.uni-heidelberg.de

Corresponding author, P. A. Vlasov: iz@chph.ras.ru

Introduction

Recent progress in the development of the chemistry of PAH formation provides a foundation for further improvement of the kinetic models of soot formation process. The main goal of the present study is the development of the detailed kinetic model of soot formation during pyrolysis of aliphatic and aromatic hydrocarbons, proposed in [1], on the basis of a comprehensive mechanism of PAH formation [2–7], the new concepts of soot nucleation and soot growth [8, 9], and recent experimental measurements of the main parameters of soot formation process [10, 11].

The Kinetic Model

In the mechanism of the gas-phase reactions, which is based on the mechanism of PAH formation in laminar premixed acetylene and ethylene flames [2] with all modifications presented in the work [3], the reactions of unsaturated aliphatic hydrocarbons with hydrogen [4, 5] and the reactions of the first ring formation from aliphatic hydrocarbons [4, 5] were added. A comprehensive set of reactions of C3-, C5-, and C7-hydrocarbons [6, 7] was also included in the gas-phase reaction mechanism. Thus, several pathways of PAH formation are incorporated in the gas-phase kinetic mechanism: (1) the alternating H-abstraction/C_2H_2 addition (HACA) route, resulting in a successive growth of PAHs, (2) the combination reactions of phenyl with C_6H_6, (3) the cyclopentadienyl recombination, and (4) the ring closure reactions of aliphatic hydrocarbons. The combination reaction of resonantly stabilized propargyl radicals, which is considered as a reversible reaction in our mechanism, is the key cyclization step in benzene formation. The modified gas-phase mechanism of the model considered consists of 2150 direct and reverse reactions between 230 different species, where the rate coefficients of some important reactions have pressure dependence. The formation, growth and coagulation of soot precursors and soot particles are described within the framework of a discrete Galerkin technique suggested by Deuflhard and Wulkow [12]. Soot precursors are formed in the reactions of polyaromatic molecules with polyaromatic radicals (starting from biphenyl P2 up to coronene A7) and in the reactions of polyaromatic radicals only (starting from cyclopentaphenanthrene and up to coronene radicals). These reactions, which can be accompanied by hydrogen abstraction, result in the formation of polyaromatic molecules, containing from 24 to 48 carbon atoms, which are stabilized by a new chemical bond. Active sites on the soot precursor particles are formed in the reactions with hydrogen atoms and OH radicals. Soot precursor particles with active sites can grow in the reactions with C_2H_2, C_4H_2, and C_6H_2, whose concentrations are rather high in pyrolysis of aliphatic and

aromatic hydrocarbons, and with polyaromatic molecules and radicals. They can coagulate and are transformed into soot particles in the reactions of the internal conversion with the formation of new chemical bonds. Soot particles can coagulate and can grow in the reactions with polyaromatic molecules and radicals. Taking into account the experimental observations presented in the works [13, 14], the polyyne sub-mechanism of soot formation, introduced in the kinetic model formulated in [1], was excluded from the soot formation model under consideration.

Results and Discussion

The results of calculations were compared with the experimental measurements of the soot yield and induction time (Figs. 1–4) determined by the cw-laser extinction technique [10, 11] and the mean radius of soot particles (Figs. 5–6) determined by the time-resolved laser-induced incandescence method [11]. As can be seen from Figs. 1–3, the new kinetic model of soot formation can adequately describe the bell-shaped temperature and concentration dependences of the soot yield in benzene and ethylene pyrolysis. For the benzene/Ar mixtures used in the work [11] (Fig. 3), the calculations demonstrate the importance of nonisothermal conditions during benzene pyrolysis and soot formation. For these mixtures, all calculations were carried out for nonisothermal conditions, when the density is constant. For the benzene/Ar and ethylene/Ar mixtures used in the work [10], this effect is negligible and the conditions are very close to isothermal ones. As can be seen from Fig. 4, the calculated induction times of soot formation in benzene pyrolysis are shorter than the experimentally measured ones. It is pertinent to mention that the novel kinetic model of soot formation considered describes quantitatively the temperature and time dependences of the mean radius of soot particles determined from the time-resolved laser-induced incandescence experiments [11] (Figs. 5, 6). The kinetic model presented in [1] significantly underestimated the mean radius of soot particles for the low temperatures of the temperature range investigated [15] and overestimated the soot yield for the high temperatures due to the contribution of the polyyne sub-mechanism [15].

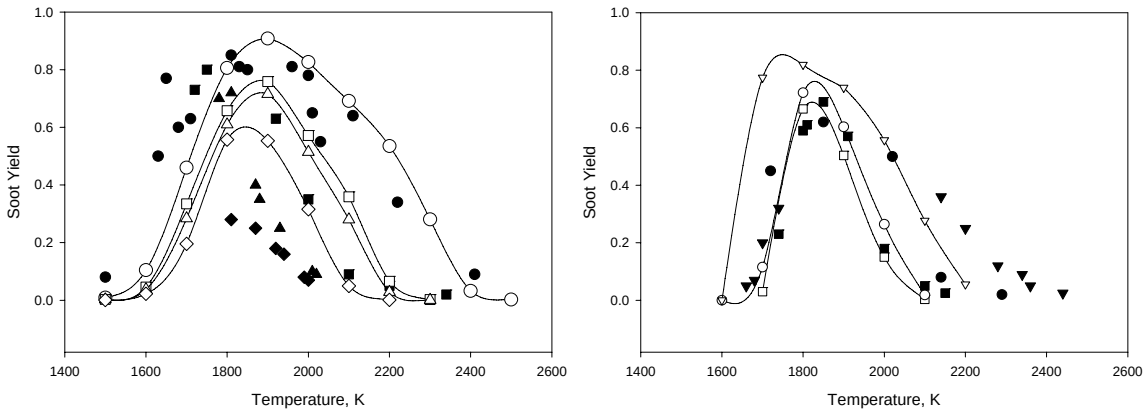

Fig. 1. Temperature dependences of the experimentally measured [10] (closed symbols) and calculated (open symbols) values of the soot yield for a fixed reaction time of t_r = 1500 μs and pressure p_5 = 50 bar for different benzene concentrations in the reactive mixture (mol/m^3): ● [C] = 4.0, ■ [C] = 1.0, ▲ [C] = 0.8, and ◆ [C] = 0.4 mol/m^3.

Fig. 2. Temperature dependences of the experimentally measured [10] (closed symbols) and calculated (open symbols) values of the soot yield for a fixed reaction time of t_r = 1500 μs and pressure p_5 = 50 bar for different ethylene concentrations in the reactive mixture (mol/m^3): ▼[C]=7.4, ● [C]=4.7, and ■ [C]=4.0 mol/m^3.

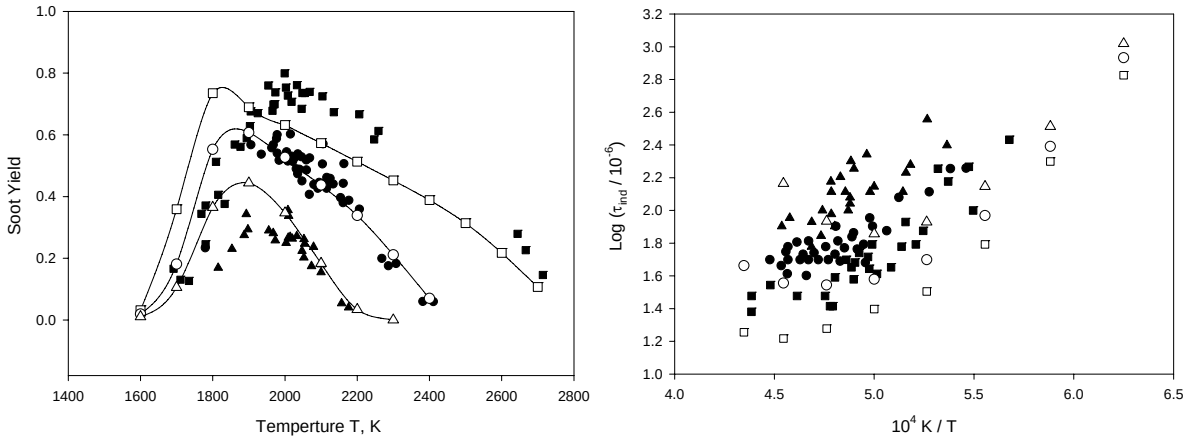

Fig. 3. Temperature dependences of the experimentally measured [11] (closed symbols) and calculated (open symbols) values of the soot yield for a fixed reaction time of t_r = 1300 μs and pressure p_5 = 1.2 bar for different benzene concentrations in the reactive mixture: (■) 2% C_6H_6, (●) 1% C_6H_6, and (▲) 0.5% C_6H_6 in Ar.

Fig. 4. Experimentally measured [11] (closed symbols) and calculated (open symbols) values of the induction time of soot particle formation for different benzene concentrations in the reactive mixture as a function of the inverse temperature: (■) 2% C_6H_6, (●) 1% C_6H_6, and (▲) 0.5% C_6H_6 in Ar, p_5 = 1.2 bar.

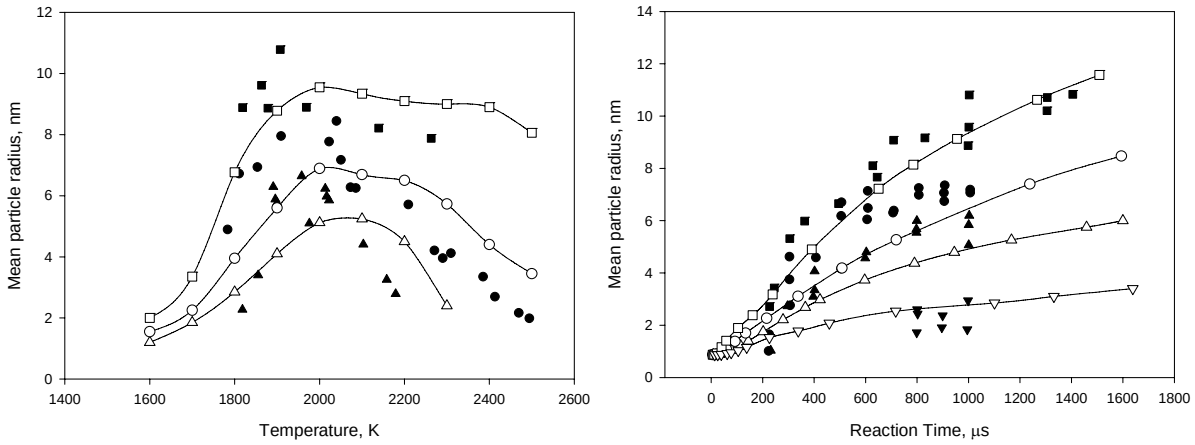

Fig. 5. Temperature dependences of the experimentally measured [11] (closed symbols) and calculated (open symbols) values of the mean soot particle radius for a fixed reaction time of t_r = 1000 μs for different benzene concentrations in the reactive mixture: (■) 2% C_6H_6, (●) 1% C_6H_6, and (▲) 0.5% C_6H_6 in Ar, p_5 = 1.2 bar.

Fig. 6. Experimentally measured [11] (closed symbols) and calculated (open symbols) values of the mean soot particle radius for different benzene concentrations in the reactive mixture as a function of the reaction time: (■) 2% C_6H_6, (●) 1% C_6H_6, (▲) 0.5% C_6H_6, and (▼) 0.25% C_6H_6 in Ar, p = 1.2 bar, T = 2000 K.

It should be noted that in [11] the values of the mean radius of soot particles were determined not only from the LII-measurements, but also, from the soot particle visualization by a high resolution transmission electron microscopy (HRTEM) method. This comparison can be regarded as a particular calibration of the time-resolved laser-induced incandescence method

and the values of the mean radius of soot particles reported in [11] can be considered as reliable ones.

Conclusions

The new detailed kinetic model of soot formation in shock tube pyrolysis of aliphatic and aromatic hydrocarbons is proposed. The model is based on the comprehensive kinetic model of PAH formation and growth, which incorporates several pathways such as the alternating H-abstraction/C_2H_2 addition (HACA) route, resulting in a successive growth of PAHs, the combination reactions of phenyl with C_6H_6, the cyclopentadienyl recombination, the ring closure reactions of aliphatic hydrocarbons, and the combination reaction of resonantly stabilized propargyl radicals. Soot precursors are formed in the reactions of polyaromatic molecules with polyaromatic radicals (starting from biphenyl up to coronene) and in the reactions of polyaromatic radicals only (starting from cyclopentaphenanthrene and up to coronene radicals). The new pathways of PAH formation introduced into the gas-phase kinetic mechanism of the soot formation model and the new concepts of soot nucleation and soot surface growth implemented in the new model made it possible to demonstrate a decisive role of PAHs in the soot inception and soot growth and to improve considerably the agreement between the results of calculations and experimental measurements.

Acknowledgments

This work was supported by the Deutsche Forschungsgemeinschaft.

References

1. P.A. Vlasov and J. Warnatz (2002) Proc. Combust. Institute **29**:2335–2341.
2. H. Wang and M. Frenklach (1997) Combust. Flame **110**:173–221.
3. J. Appel, H.Bockhorn, and M. Frenklach (2000) Combust. Flame **121**:122–136.
4. M.Frenklach, D.W. Clary, T. Yuan, W.C. Gardiner, Jr., and S.E. Stein (1986) Combust. Sci. and Tech. **50**:79–115.
5. M. Frenklach and J. Warnatz (1987) Comb. Sci. and Tech. **51**:265–283.
6. M.S. Skjøth-Rasmussen, P. Glarborg, M. Østberg, J.T. Johannessen, H. Livbjerg, A.D. Jensen, and T.S. Christensen (2004) Combust. Flame **136**:91–128.
7. H. Richter and J. B. Howard (2002) Phys. Chem. Chem. Phys. **4**:2038–2055.
8. A. Violi, G.A. Voth, and A.F. Sarofim (2004) Comb. Sci. and Tech. **176**:991–1005.
9. A. D'Alessio, A. D'Anna, P. Minutolo, L.A. Sgro, and A. Violi (2000) Proc. Combust. Institute **28**:2547–2554.
10. D. Tanke (1995) Rußbildung in der Kohlenwasserstoffpyrolyse hinter Stoßwellen // Ph.D. Thesis, Universität Göttingen.
11. R. Starke and P. Roth (2002) Combust. Flame **127**:2278–2285.
12. P. Deuflhard and M. Wulkow (1989) Impact of Computing in Science and Engineering **1:**269–301.
13. P. Weilmünster, A. Keller, and K.-H. Homann (1999) Combust. Flame **116**:62–83.
14. H. Böhm and H. Jander (1999) Phys. Chem. Chem. Phys. **1**:3775–3781.
15. I. Naydenova, M. Nullmeier, J. Warnatz, and P.A. Vlasov (2004) Comb. Sci. and Tech. **176**:1667–1703.